

# Thermal oxidative stability of perfluoropolyalkylethers and development of quantitative structure–stability relationships

K.J.L. Paciorek, S.R. Masuda, W.-H. Lin, J.H. Nakahara

Lubricating Specialties Co., Technolube Products Division, 3365 E. Slauson Avenue, Vernon, CA 90058, USA

Received 21 December 1994; accepted 23 July 1995

## Abstract

Thermal oxidative stability profiles in the presence of M-50 alloy were determined for a series of different perfluoropolyalkylether arrangements. Based on the experimental results, using molecular mechanics–molecular dynamics computations and multivariate linear regression analysis, quantitative structure–stability relationships were developed. Expression with three variables, bend, van der Waals and stretch–bend energies ( $r=0.977$ ), were shown to provide valid stability predictions. For the 10 perfluoropolyalkylethers studied, geometry-optimized molecular conformations at 313 K were determined and are presented.

**Keywords:** Perfluoropolyalkylethers; Thermal oxidative stability; Quantitative structure–stability relationships; Molecular conformation

## 1. Introduction

The high thermal oxidative stability and wide liquid ranges [1–6] associated with high molecular weights of perfluoropolyalkylethers allow these materials to be used in applications where extremes of temperature, long operation periods and high vacuum conditions prevail [7–10]. Viscosity–temperature profiles [11] and thermal oxidative stabilities, in particular in the presence of metals and/or metal alloys, are strongly dependent on the perfluoroalkylether structure [1]. Establishment of relevant quantitative structure–activity relationships (QSARs) facilitates the identification of optimum structural arrangements for given applications. This has been successfully accomplished for viscosity–temperature and viscosity–molecular weight predictions [11]. The current investigation was directed at development of structure–stability relationships, specifically thermal oxidative stability in the presence of M-50 alloy (composition: Fe, 89.72%; C, 0.83%; Cr, 4.20%; Mo, 4.25%, V, 1.00%). These conditions are dictated by the requirements of future aircraft engine lubrication systems.

## 2. Experimental details

### 2.1. Materials

The perfluoropolyalkylether fluids studied, listed in Table 1, included two commercial materials: Krytox 143AC (prod-

uct of Du Pont) and Demnum S-20 (product of Daikin Industries). The rest were experimental materials provided by the Air Force and prepared by Exfluor Research Corp. using direct fluorination of the corresponding hydrocarbon precursors [12].

### 2.2. Degradation

All the tests were carried out in pure oxygen (about 400 mmHg pressure at 25 °C) in the presence of an M-50 alloy coupon over a 24 h period at the denoted temperatures. At the end of exposure the volatile condensibles were removed in vacuo and weighed. A detailed description of the procedure and apparatus was reported previously [13]. The temperature at which the total of volatile condensibles amounted to 0.50–0.25 mg g<sup>-1</sup> (milligrams of products formed per gram of fluid employed) was defined as the degradation onset. To arrive at this point tests were carried out, if necessary, 5 °C apart. Thus the onset temperature is given within  $\pm 5$  °C.

### 2.3. Computation

The molecular mechanics calculations of energies are based on MM2 developed by Allinger [14] modified by Hypercube Inc. (MM<sup>+</sup>; HYPERCHEM 3.0 software). The MM<sup>+</sup> parameters were optimized by us using the US Air Force provided PM3 data set developed by J.J.P. Stewart specifically for perfluoroalkylethers. The bond lengths and angles

Table 1  
Fluids studied

Identification number	Fluid	Origin	Molecular weight		Degradation <sup>a</sup> temperature (°C)
			Nuclear magnetic resonance	Osmosis	
71-6	$-\text{[CF}_2\text{CF(CF}_3\text{)O]}_n-$	Krytox 143A <sup>b</sup>	6800	5400	< 288
91-21	$-\text{[CF}_2\text{CF(CF}_3\text{)O]}_n-$	F-Krytox 143AC <sup>c</sup>	7250	6000	325
88-177	$-\text{(CF}_2\text{CF}_2\text{CF}_2\text{O)}_n-$	Demnum S-20 <sup>d</sup>	2750	2500	< 300
88-177T	$-\text{(CF}_2\text{CF}_2\text{CF}_2\text{O)}_n-$	T-Demnum S-20 <sup>e</sup>			315
91-157	$-\text{[(CF}_2\text{CF}_2\text{O)}_4\text{CF}_2\text{O]}_n-$	- <sup>f</sup>	1800	2850	280
91-160	$-\text{(CF}_2\text{CF}_2\text{OCF}_2\text{O)}_n-$	- <sup>f</sup>	2800	2650	285
91-132	$-\text{[CF}_2\text{CF(CF}_3\text{)OCF}_2\text{CF(CF}_3\text{)OCF}_2\text{O]}_n-$	- <sup>f</sup>	2700	3050	300
91-161	$-\text{(CF}_2\text{CF}_2\text{O)}_n-$	- <sup>f</sup>	2450	3000	310
91-158	$-\text{[CF}_2\text{CF(CF}_2\text{OCF}_2\text{CF}_2\text{OCF}_2\text{CF}_2\text{OCF}_3\text{)O]}_n-$	- <sup>f</sup>	5650	3950	310
91-105	$-\text{(CF}_2\text{CF}_2\text{CF}_2\text{CF}_2\text{OCF}_2\text{O)}_n-$	- <sup>f</sup>	2700	2500	310
91-106	$-\text{(CF}_2\text{CF}_2\text{CF}_2\text{CF}_2\text{CF}_2\text{OCF}_2\text{O)}_n-$	- <sup>f</sup>	2800	2500	310
91-126	$-\text{(CF}_2\text{CF}_2\text{CF}_2\text{CF}_2\text{O)}_n-$	- <sup>f</sup>	3100	2600	315

<sup>a</sup> This is the degradation onset temperature at which volatile condensibles amounted to  $0.5 \pm 0.25 \text{ mg g}^{-1}$ .

<sup>b</sup> Product of DuPont.

<sup>c</sup> Krytox 143AC which was subjected to fluorination at elevated temperatures [12].

<sup>d</sup> Product of Daikin Industries.

<sup>e</sup> Demnum S-20 which was exposed to oxygen at 315 and 330 °C in the presence of M-50 alloy for consecutive 24 h periods.

<sup>f</sup> All of these fluids were prepared by direct fluorination of their hydrocarbon precursors [12].

used are as follows: C–C, 1.554 Å; C–O, 1.354 Å; C–F, 1.312 Å; C–C–C, 112.2°; C–C–O, 108.2°; C–O–C, 124.7°; O–C–O, 109.4°. For valid derivations, based partially on the average molecular weights of the fluids studied (the exception being Krytox 143AC and its fluorinated product), all the computations were carried out on representative telomers having molecular weights as closely as feasible to 2500. Each of the structures listed in Table 2 was geometry optimized at 0 K. Using the program's molecular dynamics the temperature was increased to 313 K over 3 ps. After equilibrium, over 5 ps, data were collected over the next 2 ps for a total of 2000 data points. The conformations obtained at 0, 1, 1.5 and 2 ps were geometry optimized and the energy parameters, subsequently calculated at the four time periods, were averaged. These are the energy parameters listed in Table 2. The

regression analyses to develop the QSARs were performed with SPSS 4.01 computer program.

### 3. Results and discussion

The present study, as mentioned earlier, involved two commercial fluids, Krytox 143AC  $-\text{[CF(CF}_3\text{)CF}_2\text{O]}_n-$  and Demnum S-20  $-\text{[CF}_2\text{CF}_2\text{CF}_2\text{O]}_n-$ , as well as a series of perfluoropolyalkylether experimental fluids [12]. None of these materials is unimolecular; all consist of telomer mixtures owing to the nature of the synthesis. The end groups tend to vary. These aspects were discussed earlier [11]. It is believed that insofar as stability is concerned the nature of the end groups, whether  $\text{CF}_3\text{O}$ ,  $\text{C}_2\text{F}_5\text{O}$ ,  $\text{C}_3\text{F}_7\text{O}$ , is of a minor

Table 2  
Perfluoropolyalkylether energy components listing

Structure	Energy components <sup>a</sup> (kcal mol <sup>-1</sup> )					
	BOND	BEND	DIHED	VDW	SB	ES
$\text{CF}_3\text{O}[(\text{CF}_2\text{CF}_2\text{O})_4\text{CF}_2\text{O}]_4\text{CF}_3$	12.65	13.75	-114.6	-10.17	1.73	226.9
$\text{CF}_3\text{O}(\text{CF}_2\text{CF}_2\text{OCF}_2\text{O})_{13}\text{CF}_3$	10.20	14.66	-106.9	-5.87	1.61	189.7
$\text{CF}_3\text{O}[\text{CF}_2\text{CF(CF}_3\text{)OCF}_2\text{CF(CF}_3\text{)OCF}_2\text{O}]_6\text{CF}_3$	18.09	21.41	-104.0	-23.13	2.57	270.1
$\text{CF}_3\text{O}(\text{CF}_2\text{CF}_2\text{O})_{26}\text{CF}_3$	15.66	15.16	-135.7	0.02	2.04	284.9
$\text{CF}_3\text{O}[\text{CF}_2\text{CF(CF}_2\text{OCF}_2\text{CF}_2\text{OCF}_2\text{CF}_2\text{OCF}_3\text{)O}]_5\text{CF}_3$	14.77	23.08	-101.2	-14.01	2.16	244.3
$\text{CF}_3\text{O}(\text{CF}_2\text{CF}_2\text{CF}_2\text{CF}_2\text{OCF}_2\text{O})_8\text{CF}_3$	21.99	17.03	-125.1	-9.29	2.48	324.9
$\text{CF}_3\text{O}(\text{CF}_2\text{CF}_2\text{CF}_2\text{CF}_2\text{OCF}_2\text{O})_7\text{CF}_3$	25.93	18.04	-133.4	-12.64	2.90	373.2
$\text{CF}_3\text{O}(\text{CF}_2\text{CF}_2\text{CF}_2\text{O})_{14}\text{CF}_3$	24.58	17.04	-145.3	-0.97	2.34	382.0
$\text{CF}_3\text{O}(\text{CF}_2\text{CF}_2\text{CF}_2\text{O})_{11}\text{CF}_3$	29.80	18.35	-156.4	-6.68	2.88	442.8
$\text{CF}_3\text{O}[\text{CF}_2\text{CF(CF}_3\text{)O}]_{14}\text{CF}_3$	20.41	21.12	-116.9	-5.24	2.54	316.8

<sup>a</sup> BOND, bonding energy; BEND, bending energy; DIHED, torsion energy; VDW, van der Waals energy; SB, stretch–bend energy; ES, electrostatic energy.

importance compared with the effect of the types of the repeating segments [1,11]. It must be stressed that perfluoropolyalkylethers exhibit very high thermal oxidative stability in the absence of metals, i.e. when exposed to high temperatures in oxygen in glass. However, metals promote greatly fluids' degradation [1] and lower significantly the degradation onset. In view of the envisioned application, namely a contact of the fluid at elevated temperatures with components manufactured from M-50 alloy, all the evaluations were carried out in the presence of this material.

From the data presented in Fig. 1 it is apparent that the commercial fluids, Krytox and Demnum, contain impurities which lower the degradation onset compared with materials given stabilization treatment. It has been established that in Krytox fluids the impurities responsible for the decreased stability consist of hydrogen-terminated chains  $-\text{OCF}(\text{CF}_3)\text{H}$  [1,15]. The nature of the impurities in Demnum is unknown, although in view of the synthesis process [4] residual hydrogen is again suspected. In both instances pretreatment at 316–330 °C in oxygen, in the presence of M-50 alloy, degrades the low stability chains into volatile products which are then removed. Fluorination provides another

way to remove residual hydrogen and was successfully employed in the case of Krytox fluid [12].

It would appear from the degradation profiles shown in Fig. 1 that the inherent thermal oxidative stability of a branched poly(hexafluoropropene oxide) is higher than that of its linear analogue i.e. at 315 °C the degradation value for  $-\text{CF}(\text{CF}_3)\text{CF}_2\text{O}-$  was found to be  $0.03 \text{ mg g}^{-1}$  vs.  $0.70 \text{ mg g}^{-1}$  for  $-(\text{CF}_2\text{CF}_2\text{CF}_2\text{O})_n-$ .

As noted earlier all the other fluids studied were obtained by direct fluorination of their hydrocarbon precursors. No difference was observed in the degradation onset of hydrogen-free  $-\text{CF}(\text{CF}_3)\text{CF}_2\text{O}-$  prepared by hexafluoropropene oxide telomerization and that of the compound obtained by direct fluorination of poly(propylene oxide) (Fig. 2) confirming that stability is inherent in a given structure and proving the validity of the experimental approach. It is the weakest link or unit which determines the stability of the given material. This is illustrated by the comparison of the degradation onset of 310 °C, determined for  $-(\text{CF}_2\text{CF}_2\text{O})_n-$  and for  $-\text{CF}_2\text{CF}(\text{CF}_2\text{OCF}_2\text{CF}_2\text{OCF}_2\text{CF}_2\text{OCF}_3)\text{O}-$ , as shown in Figs. 2 and 3. In the second material the sequence of tetrafluoroethylene oxide groups provides the instability site.

Introduction of a difluoroformyl group into the octafluorobutene oxide system,  $-(\text{CF}_2\text{CF}_2\text{CF}_2\text{CF}_2\text{O})_n-$ , to give the  $-(\text{CF}_2\text{CF}_2\text{CF}_2\text{CF}_2\text{OCF}_2\text{O})_n-$  structure, lowers the degradation onset by 5 °C, from 315 °C to 310 °C, as shown in Fig. 4. An increase in the number of adjacent  $\text{CF}_2$  groups from 4 to 5 has no effect on the degradation onset as evident from the plots in Fig. 4. It is of interest that  $-(\text{CF}_2\text{CF}_2\text{CF}_2\text{O})_n-$  and  $-(\text{CF}_2\text{CF}_2\text{CF}_2\text{CF}_2\text{O})_n-$  arrangements exhibit essentially identical degradation profiles (Fig. 4). Apparently it requires at least three adjacent  $\text{CF}_2$  groups to inhibit the "activity" effect of oxygen. Studies performed on aromatic-perfluoroalkylether compounds support these observations [16].

It is unexpected that the introduction of difluoroformyl groups into the hexafluoropropene oxide system decreases the degradation onset by 25 °C (see Fig. 2) vs. 5 °C for the

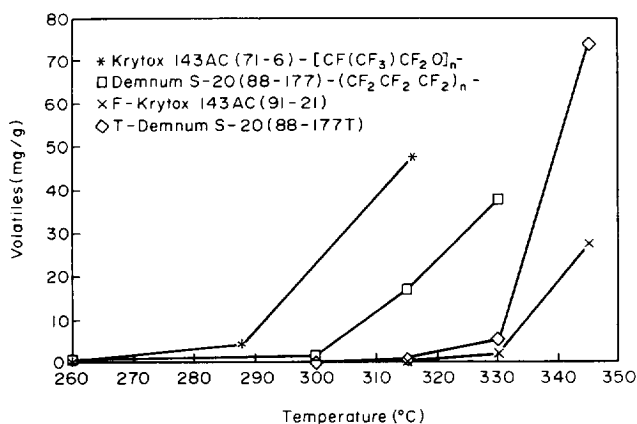


Fig. 1. Comparison of thermal oxidative behavior of as-received commercial fluids with pretreated materials.

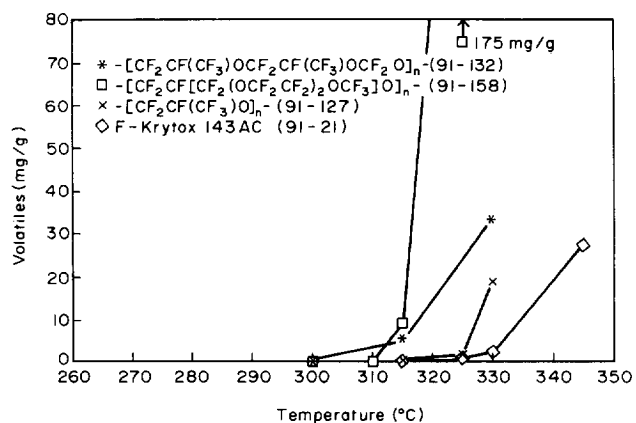


Fig. 2. Effect of the presence of difluoroformyl groups and tetrafluoroethylene oxide branching on the thermal oxidative stability of poly(hexafluoropropene oxide).

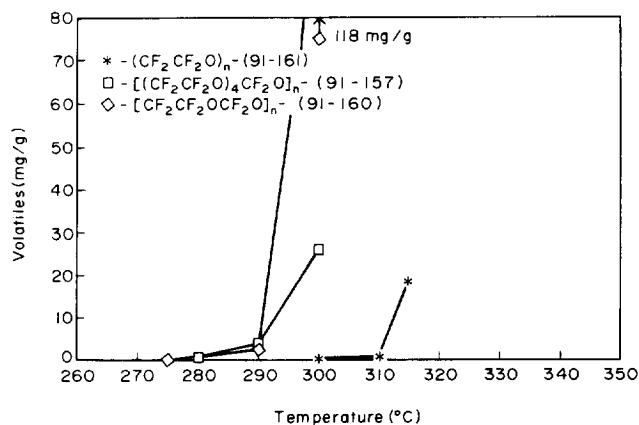


Fig. 3. Effect of the presence and relative proportions of difluoroformyl groups on the thermal oxidative stability of poly(tetrafluoroethylene oxide) fluids.

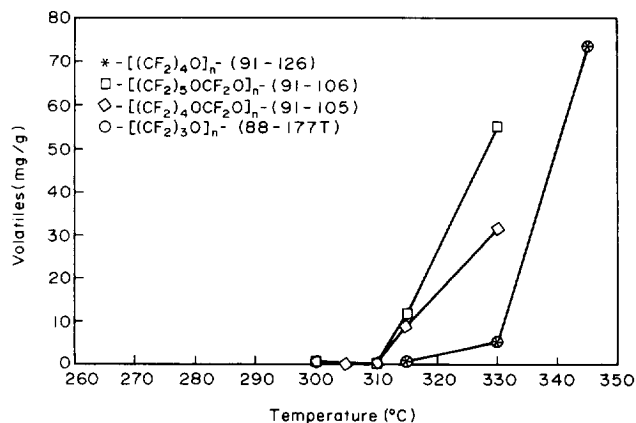


Fig. 4. Effect of difluoroformyl groups on thermal oxidative behavior of perfluoropolyalkylethers containing 4 and 5 adjacent difluoromethylene groups.

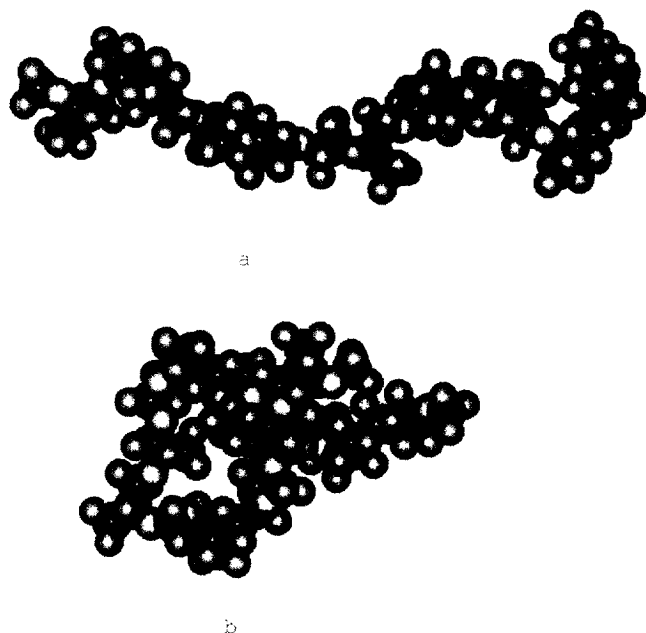


Fig. 5. Geometry-optimized conformations after molecular dynamics at 40 °C: (a)  $\text{CF}_3\text{O}[\text{CF}_2\text{CF}(\text{CF}_3)\text{O}]_{14}\text{CF}_3$ ; (b)  $\text{CF}_3\text{O}[\text{CF}_2\text{CF}(\text{CF}_3)\text{OCF}_2\text{CF}(\text{CF}_3)\text{OCF}_2\text{O}]_6\text{CF}_3$ .

octafluorobutene oxide structure. Furthermore, the actual onset temperature (300 °C) is lower for the copolymer  $-\text{CF}_2\text{CF}(\text{CF}_3)\text{OCF}_2\text{CF}(\text{CF}_3)\text{OCF}_2\text{O}-$  than the 310 °C determined for  $-(\text{CF}_2\text{CF}_2\text{CF}_2\text{CF}_2\text{OCF}_2\text{O})_n-$  (Fig. 4). It is possible that the presence of the  $-\text{OCF}_2-$  unit disrupts the protective shielding of trifluoromethyl groups and the arrangement approximates more closely a two-carbon environment represented by, for example, poly(tetrafluoroethylene oxide).

The presence of difluoroformyl groups in the tetrafluoroethylene oxide systems results in a drastic drop of the degradation onset from 310 °C to 280–285 °C. The degradation onsets for the two materials investigated  $-(\text{CF}_2\text{CF}_2\text{OCF}_2\text{O})_n-$  and  $-(\text{CF}_2\text{CF}_2\text{O})_4\text{CF}_2\text{O}-$  are virtually identical. However, the subsequent rate of degradation

above this threshold is significantly higher for the composition having the higher difluoroformyl proportion as evident from the plots in Fig. 3.

Based on earlier work [1] and the current investigations it is obvious that there is a definite interdependence between

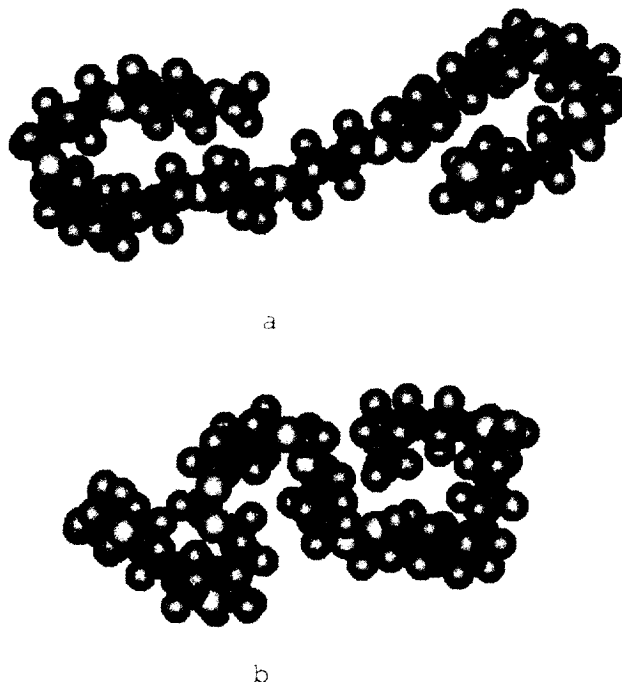


Fig. 6. Geometry-optimized conformations after molecular dynamics at 40 °C: (a)  $\text{CF}_3\text{O}(\text{CF}_2\text{CF}_2\text{CF}_2\text{CF}_2\text{O})_{11}\text{CF}_3$ ; (b)  $\text{CF}_3\text{O}(\text{CF}_2\text{CF}_2\text{CF}_2\text{CF}_2\text{OCF}_2\text{O})_8\text{CF}_3$ .

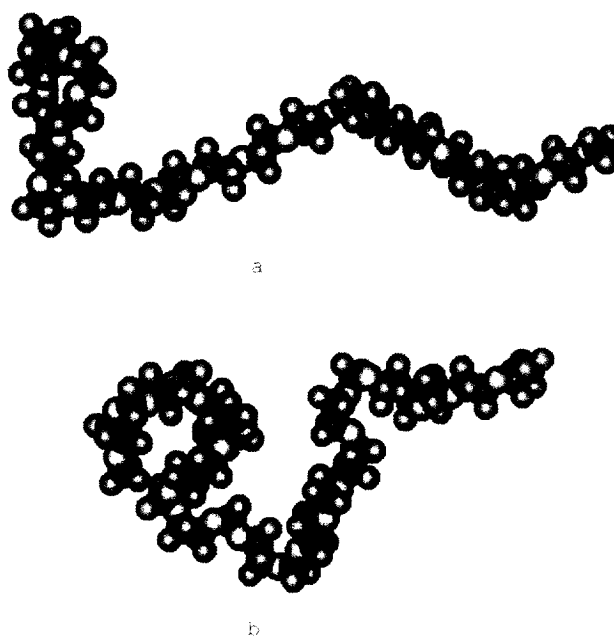


Fig. 7. Geometry-optimized conformations after molecular dynamics at 40 °C: (a)  $\text{CF}_3\text{O}(\text{CF}_2\text{CF}_2\text{O})_{20}\text{CF}_3$ ; (b)  $\text{CF}_3\text{O}(\text{CF}_2\text{CF}_2\text{OCF}_2\text{O})_{13}\text{CF}_3$ .

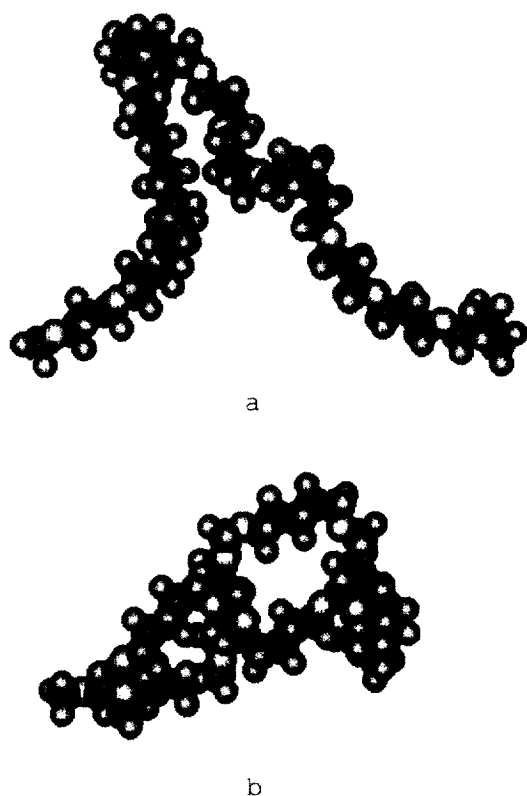


Fig. 8. Geometry-optimized conformations after molecular dynamics at 40 °C: (a)  $\text{CF}_3\text{O}(\text{CF}_2\text{CF}_2\text{CF}_2\text{O})_{14}\text{CF}_3$ ; (b)  $\text{CF}_3\text{O}(\text{CF}_2\text{CF}_2\text{CF}_2\text{-CF}_2\text{CF}_2\text{OCF}_2\text{O})_7\text{CF}_3$ .

structure and the thermal oxidative stability of perfluoroalkylethers. Establishment of QSARs to be utilized in conjunction with the previously developed quantitative structure–viscosity relationships [11] should allow us to identify the best perfluoroalkylether arrangement for a given application without having to synthesize and evaluate a series of potential candidates. A structure–stability correlation based on energy parameters provides a meaningful approach. Although the perfluoropolyalkylethers studied are mixtures of telomers the use of unimolecular compositions in the computational treatments seemed reasonable in view of the results obtained in the structure–viscosity studies. A catalytic process, which is the case for the M-50-promoted degradations, must be dependent on juxtaposition of units or segments in a given material. This is of a particular importance in high molecular weight systems when in a single molecule a number of different configurations can exist. To permit the various molecular orientations freedom of motion is necessary. In a computational treatment this can be achieved by imparting energy (velocity) to molecular conformations (obtained using molecular mechanics). Arbitrarily, we have selected 313 K as the temperature at which the various energy components, given in Table 2, were computed after geometry optimizations. These are average values of four different conformations. Representative conformations of the perfluoropolyalkylethers, listed in Table 2, are presented in Figs. 5–9.

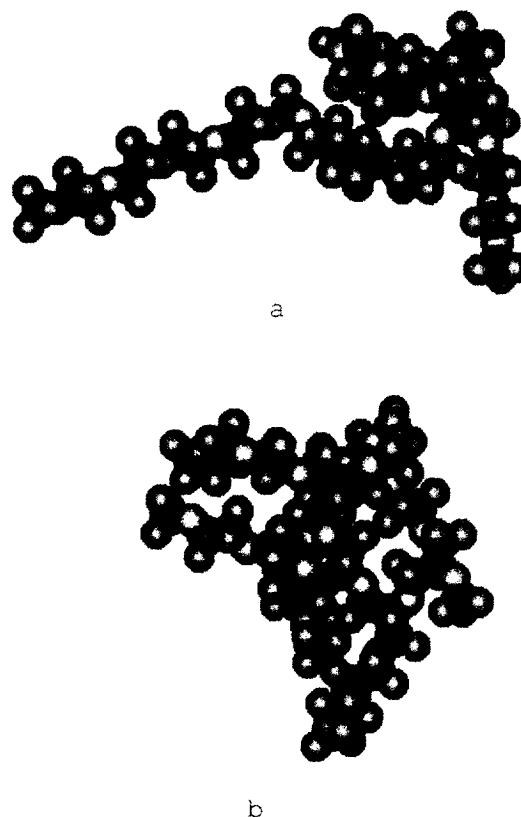


Fig. 9. Geometry-optimized conformations after molecular dynamics at 40 °C: (a)  $\text{CF}_3\text{O}[(\text{CF}_2\text{CF}_2\text{O})_4\text{CF}_2\text{O}]_4\text{CF}_3$ ; (b)  $\text{CF}_3\text{O}[\text{CF}_2\text{CF}_2\text{-(CF}_2\text{OCF}_2\text{CF}_2\text{OCF}_2\text{CF}_2\text{OCF}_3)\text{O}]_5\text{CF}_3$ .

The lack of uniformity in the structural arrangements illustrates the points discussed above.

To develop QSAR expressions the energy components given in Table 2 were employed in multivariate linear regression analyses. The equations, derived using different energy parameters, together with the corresponding Pearson correlation coefficients  $r$  are presented in Table 3. Employing just three descriptors gives an  $r$  of 0.977 and an  $s$  (standard error of estimate) of 3.61. The graphical presentation is depicted in Fig. 10. To determine the validity of this approach, equations using the three energy components, namely bending, van der Waals and stretch–bend energies, were derived employing 9 out of the 10 fluids. The degradation temperature of the excluded fluid was then calculated. This operation was performed for each of the 10 fluids. The relevant data are compiled in Table 4. The agreement between calculated and actual degradation temperature is illustrated in Fig. 11.

Based on these results and the earlier-developed viscosity–structure correlations [11] it is apparent that it is feasible to design a perfluoropolyalkylether system having specific stability and viscosity characteristics. It must be stressed that unfortunately [1,11] perfluoropolyalkylethers exhibiting the highest thermal oxidative stabilities possess also the poorest viscosity–temperature profiles. Thus an optimum composition for a given application will have to be a compromise system.

Table 3  
Quantitative structure–activity relationship expressions based on energy descriptors

Number of variables	$r^a$	$s^b$	Variable coefficients <sup>c</sup>						Constant
			BOND	BEND	DIHED	VDW	SB	ES	
6	0.982	4.48	-1.37	2.38	0.16	1.72	29.98	0.08	231.7
5	0.982	3.89	-0.70	2.59	0.05	1.75	29.74		225.4
4	0.982	3.50	-0.84	2.68		1.71	30.09		219.3
3	0.977	3.61		3.00		1.52	17.32		225.2
2	0.860	8.05		4.34		1.56			241.8
2	0.841	8.54					26.24		253.2
2	0.749	10.44		1.18			18.30		242.9

<sup>a</sup>  $r$  is the Pearson correlation coefficient.

<sup>b</sup>  $s$  is the standard error.

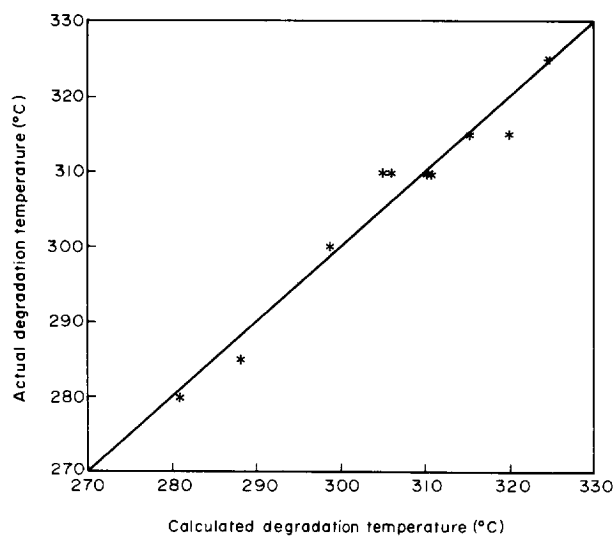
<sup>c</sup> BOND, bonding energy; BEND, bending energy; DIHED, torsion energy; VDW, van der Waals energy; SB, stretch–bend energy; ES, electrostatic energy.

Table 4  
Degradation temperatures calculated from equations derived from data excluding the fluid of interest

Fluid excluded	$r^a$	Variable <sup>b</sup> coefficients			Constant	Degradation temperature (°C)	
		BEND	VDW	SB		Calculated	Actual
CF <sub>3</sub> O[(CF <sub>2</sub> CF <sub>2</sub> O) <sub>4</sub> CF <sub>2</sub> O] <sub>4</sub> CF <sub>3</sub>	0.961	2.88	1.47	16.89	228.2	280	282
CF <sub>3</sub> O(CF <sub>2</sub> CF <sub>2</sub> OCF <sub>2</sub> O) <sub>13</sub> CF <sub>3</sub>	0.975	2.93	1.50	15.34	231.5	285	290
CF <sub>3</sub> O[CF <sub>2</sub> CF(CF <sub>3</sub> )OCF <sub>2</sub> CF(CF <sub>3</sub> )OCF <sub>2</sub> O] <sub>6</sub> CF <sub>3</sub>	0.978	3.00	1.62	17.29	225.9	300	297
CF <sub>3</sub> O(CF <sub>2</sub> CF <sub>2</sub> O) <sub>20</sub> CF <sub>3</sub>	0.984	3.02	1.41	17.76	222.2	310	304
CF <sub>3</sub> O[CF <sub>2</sub> CF(CF <sub>2</sub> OCF <sub>2</sub> CF <sub>2</sub> OCF <sub>2</sub> CF <sub>2</sub> OCF <sub>3</sub> )O] <sub>5</sub> CF <sub>3</sub>	0.977	3.15	1.52	16.62	224.3	310	312
CF <sub>3</sub> O(CF <sub>2</sub> CF <sub>2</sub> CF <sub>2</sub> CF <sub>2</sub> OCF <sub>2</sub> O) <sub>8</sub> CF <sub>3</sub>	0.985	3.18	1.55	16.27	224.2	310	304
CF <sub>3</sub> O(CF <sub>2</sub> CF <sub>2</sub> CF <sub>2</sub> CF <sub>2</sub> OCF <sub>2</sub> O) <sub>7</sub> CF <sub>3</sub>	0.977	2.97	1.51	17.58	225.1	310	311
CF <sub>3</sub> O(CF <sub>2</sub> CF <sub>2</sub> CF <sub>2</sub> O) <sub>14</sub> CF <sub>3</sub>	0.976	3.00	1.52	17.35	225.2	315	315
CF <sub>3</sub> O(CF <sub>2</sub> CF <sub>2</sub> CF <sub>2</sub> CF <sub>2</sub> O) <sub>11</sub> CF <sub>3</sub>	0.988	2.86	1.57	20.45	221.6	315	322
CF <sub>3</sub> O[CF <sub>2</sub> CF(CF <sub>3</sub> )O] <sub>14</sub> CF <sub>3</sub>	0.970	2.96	1.50	17.34	225.7	325	324

<sup>a</sup>  $r$  is the Pearson correlation coefficient.

<sup>b</sup> BEND, bending energy; VDW, van der Waals energy; SB, stretch–bend energy.



$$T_{\text{Deg}} = 3.00(\text{BEND}) + 1.52(\text{VDW}) + 17.32(\text{S-B}) + 225.22 \quad r = 0.977$$

Fig. 10. Plot of calculated vs. actual degradation temperature as a function of bending, van der Waals and stretch–bend energies.

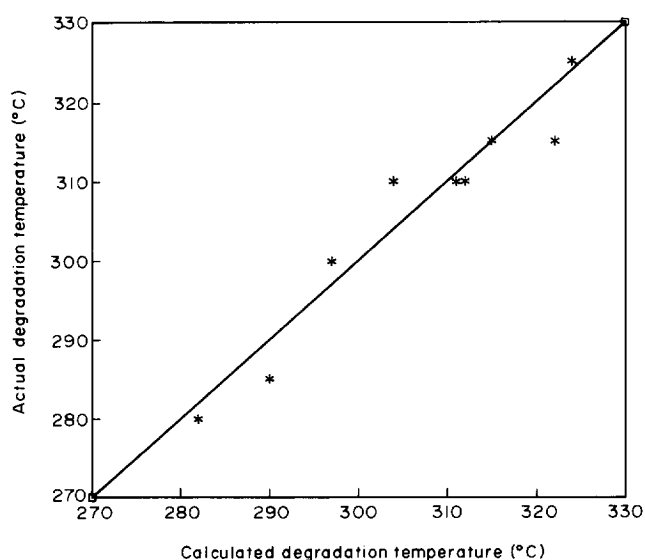


Fig. 11. Plot of calculated vs. actual degradation temperatures obtained from equations derived excluding the fluid of interest.

## Acknowledgments

We wish to acknowledge the support of US Air Force, Wright Laboratory–Materials Directorate for this work under Contract F33615-89-C-5646 and we wish to thank Dr. W.M. Warner for helpful discussions.

## References

- [1] K.J.L. Paciorek and R.H. Kratzer, *J. Fluorine Chem.*, 67 (1994) 169.
- [2] W.H. Gumprecht, *ASLE Trans.*, 9 (1966) 24.
- [3] D. Sianesi, A. Pasetti and G. Belardinelli, *US Patent 3,715,378*, 1973.
- [4] Y. Ohsaka, T. Tohzuka and S. Takaki, *Eur. Patent Appl. 0,148,482*, 1984.
- [5] W.R. Jones, Jr., The properties of perfluoropolyethers used for space applications, *NASA Tech. Memo. 106275*, 1993.
- [6] K. Johns, C. Corti, L. Montagna and P. Srinivasan, *J. Phys. D*, 25 (1992) A141.
- [7] G. Caporiccio, C. Corti, S. Saldini and G. Carniselli, *Ind. Eng. Chem. Prod. Res. Dev.*, 21 (1982) 515.
- [8] J.F. Moulder, J.S. Hammond and K.L. Smith, *Appl. Surf. Sci.*, 25 (1986) 445.
- [9] N.D. Watson et al., Earth radiation budget experiment (ERBE) scanner instrument anomaly investigation, *NASA Tech. Memo. 8736*, 1985.
- [10] W. Morales and W.R. Jones, Jr., Analysis of spacecraft instrument ball bearing assembly lubricated by a perfluoroalkylether, *NASA Tech. Memo. 87260*, 1986.
- [11] K.J.L. Paciorek, S.R. Masuda, W.-H. Lin and J.H. Nakahara, *J. Fluorine Chem.*, 73 (1995) 33.
- [12] T.R. Bierschenk, H. Kawa, T.J. Juhlke and R.J. Lagow, Perfluoropolyalkylether base fluids, *US Air Force Rep. WL-TR-91-4120*, 1992.
- [13] K.J.L. Paciorek, R.H. Kratzer, J. Kaufman and J.H. Nakahara, *J. Appl. Polym. Sci.*, 24 (1979) 1397.
- [14] N.L. Allinger, *J. Am. Chem. Soc.*, 99 (1977) 8127.
- [15] K.J.L. Paciorek, T.I. Ito and R.H. Kratzer, Thermal oxidative degradation reactions of perfluoroalkylethers, *NASA Rep. CR-165516*, 1981.
- [16] K.J.L. Paciorek, unpublished results.